World Sustainable Energy Days 2020
Young Energy Researchers Conference
March 4 – 6 2020, Wels, Austria

NEW CASCADE DESIGN TECHNIQUE FOR HIGHER EFFICIENCY ORC SYSTEMS

Noémie Chagnon-Lessard*, Louis Gosselin

Department of Mechanical Engineering, Université Laval, Quebec City, QC, Canada
*Corresponding author. noemie.chagnon-lessard.1@ulaval.ca.

ABSTRACT

Increasing the energy efficiency of systems converting heat to power is an effective way of reducing our greenhouse gas emissions. The Organic Rankine Cycle (ORC) is one of the most performant cycles for medium/low-temperature renewable heat source power plants and waste heat recovery applications. The "cascade method", a new design technique that optimizes all the heat transfer interactions in one step, was tested with three different cases. No assumptions on the internal heat recovery architecture are required. This paper shows step-by-step how to generate the architecture from the optimization results. In one case, the method provided a 40% increase of the power produced. The method was also shown to work well when two hot sources are considered simultaneously, as in one of the test cases.

KEYWORDS: Organic Rankine Cycle, Energy Efficiency, Waste Heat Recovery, Optimization, Pinch Analysis.

LIST OF ABBREVIATIONS

CO	condenser
EC	economizer
EV	evaporator
GWP	global warming potential
HEN	heat exchanger network
ODP	ozone depletion potential
ORC	Organic Rankine Cycle
PP	feed pump
REC	recuperator
SH	superheater
TB	turbine

1. Introduction

Some authors estimate that as much as three quarters of the energy that humankind produces ends up as waste heat [1]. A large number of applications can be found in which heat is a byproduct, ultimately dissipated into the environment. In fact, waste heat sources can be "visible" is many systems of the utmost importance in our modern societies (e.g., exhaust of combustion engines, industrial chimneys, cooling towers from buildings, datacenters, etc.). In a world in which we are trying to move towards renewable and low-carbon energy sources, recovering waste heat offers a tremendous potential for reducing our energy consumption and thus, our environmental footprint. Because of the large amounts of available waste heat, recovering even a small fraction of them can drastically boost our overall energy efficiency.

Organic Rankine cycles (ORCs) are among the most effective cycles for converting low to medium temperature heat sources (such as typical waste heat sources) into electricity. ORCs are also particularly attractive for renewable heat sources, such as geothermal and solar energy. Because their efficiency is limited (10% of the available heat can typically be converted to electricity, and not higher than 24% for high temperature applications [2]) and their cost can be high, there is a need for adapting and optimizing as much as possible the architecture, design and operation of ORCs for specific applications. For example, literature reveals that the best ORC design strongly depends on the hot and cold source temperature [3]. Furthermore, the performance of ORC is directly related to the choice of working fluid.

The Rankine cycle is the basic steam cycle for power generation. The ORC is a Rankine cycle using an organic fluid (e.g. R134a, propane, etc.) instead of water as working fluid, usually more suitable for heat sources with lower temperatures. Its most simple version involves four evolutions of the working fluid. Starting from saturated liquid (a state situated on the left curve in a thermodynamic diagram), the fluid reaches the desired evaporating pressure through a pump. Heat exchangers, typically an economizer, evaporator and superheater, heat the fluid at constant pressure until it achieves a gaseous state. A turbine produces mechanical work by expending it, and finally, the fluid returns to the initial saturated liquid state by transferring heat at constant pressure to a cold sink through a condenser.

Different types of ORCs have been proposed and studied in literature. To increase the overall efficiency, ORCs can

comprise internal energy recovery techniques that help preheating the fluid after the pump. For example, regeneration [4] extracts a fraction of the fluid at an intermediate stage of the turbine, and recuperation [5] transfers heat from the turbine outlet with a recuperator. The heat exchange from the heat source may also have variations. The fluid at the turbine outlet can be heated once more to expand in a second turbine with reheating [6], or its flow rate can be divided to be heated at two different pressures with the dual-pressure heating [7]. For each of these ORC types, there is also a number of parameters to choose, such as the operating pressures and temperatures, the working fluid, etc.

Because of the large number of possibilities, it is always difficult to identify the "best" ORC for a given application. Our group is involved in the development of new ORC design methods to remedy this situation. One particular challenge that we face when designing an ORC is to establish the maximal achievable internal heat recovery in the cycle. On this matter, [8] proposes to separate the heat exchange interactions from the basic topology (turbine(s) and pump(s) in the case of ORCs) and to include them in a "black box" that can be optimized. Authors of [9] refer to this principle as the "Heatsep" method, where the heat transfer network in the black box (the number of heat exchangers and their inter-connections) is defined after the optimization. The present paper seeks to evaluate the potential of this new method for the optimization of ORCs internal design through three different case studies. The shifting technique for pinch analysis and the heat cascade method [10] are employed to evaluate the energy balance in the heat transfer network. For concision, the combination of Heatsep, shifting, and heat cascade methods is labeled here as the "cascade method".

This paper presents in Section 2 the methodology behind the simulation and optimization of ORCs using the cascade method. Then, three case studies explain how to use the optimization results to generate the internal design of the ORC architecture: ORC with reheat (Section 3) and dual-pressure heating ORC with one heat source (Section 4) and two heat sources (Section 5).

2. Modeling of ORC with cascade method

An example of the ORC analyzed in this paper is shown in Fig. 1a, with states {1} to {9} identified on the T-s diagram. The hot source available at $T_{h,i}$ transfers heat to the ORC and then its temperature goes down to $T_{h,o}$. Note that the other flow rates and the ORC net power output are expressed with respect to the flow rate of this hot stream $\dot{m}_h$. The cold source has an inlet temperature $T_{c,i}$ and an outlet temperature $T_{c,o}$, with a flow rate ratio $R_c = \dot{m}_c/\dot{m}_h$.

The model relies on a series of assumptions:

- The system is assumed to operate in steady-state. The inlet of the hot and cold sources is fixed at $T_{h,i}$ and $T_{c,i}$.
- Pressure losses and heat losses are negligible.
- Turbines and pump(s) have assigned isentropic efficiency η_{TB} and η_{PP} of 0.85 and 0.8, respectively.
- Cooling system specific work consumption (see last term of Eq. (1)) is calculated using a cooling efficiency η_c of 1/60, an estimated value based from a previous work on ORCs employing a wet cooling tower [11].
- Only subcritical ORCs are taken into account in this study.
- All heat exchangers have a counterflow configuration.

The ORC shown in Fig. 1a includes reheating: the working fluid is heated in a series of heat exchangers, is expanded in a first turbine TB1 from P_H to P_I, is reheated, and then is expended through a second turbine TB2 from P_I to P_L. The flow rate ratio of the working fluid is $R_{wf} = \dot{m}_{wf}/\dot{m}_h$.

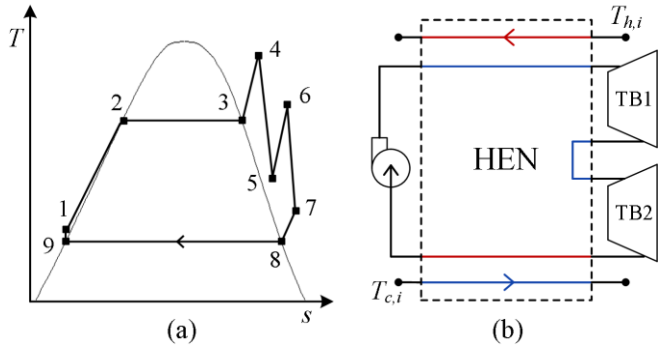

Figure 1. (a) Example of ORC cycle with reheat on a T-s diagram. (b) Black box delineating the position of the heat exchanger network (HEN).

The objective function to maximize is the net specific work output, which in the example of Fig. 1 can be written as

$$w = R_{wf}\left[\left(h_4 - h_5\right) + \left(h_6 - h_7\right) - \left(h_1 - h_9\right)\right] - \eta_c R_c \left(h_{c,o} - h_{c,i}\right) \quad (1)$$

This expression is obtained by subtracting the parasitic load (pumping and cooling work consumption) from the work produced in the turbines.

Another objective function employed in this work is the exegertic efficiency η_{ex} also known as second-law efficiency. The definition chosen [12] in this work is

$$\eta_{ex} = \frac{e_W}{\left(e_W\right)_{rev}} = \frac{w}{h_{h,i} - h_{h,o} - T_{c,i}\left(s_{h,i} - s_{h,o}\right)} \quad (2)$$

where e_W is the specific flow exergy and s the entropy. This is thus the amount of useful mechanical power divided by the flow exergy contained in the hot source.

No details regarding the internal heat recovery strategy (or its absence) is specified at this point. Similarly, no information is given on how the heat from the hot source is delivered to the ORC or how the heat is dissipated in the cold source stream (e.g., number of heat exchangers, stream splitting, etc.).

As proposed by [8], a black box to be filled with a heat exchanger network (HEN) is delineated in the system of Fig. 1a and is reported in Fig. 1b with the different streams piercing this black box. Streams containing a phase change must be broken down to separate the evaporation or condensation, the compressed liquid state, and superheated gas state due to the discrepancy of their thermal properties. It can be seen that in this example, there are three hot streams (i.e., streams to be cooled), namely the hot source fluid from $T_{h,i}$ to $T_{h,o}$ and the working fluid from state {7} to state {8} (superheated gas part) and from state {8} to state {9} (condensation part). Similarly, there are five cold streams (i.e., streams to be heated). Four of these five streams are working fluid streams, i.e., compressed liquid states {1} to {2}, evaporation from states {2} to {3}, and superheated gas states {3} to {4} and {5} to {6}. The fifth cold stream is the cold source fluid, going from $T_{c,i}$ to $T_{c,o}$. The questions are thus to establish the maximal possible performance of the HEN in the black box of Fig. 1b and the resulting equipment architecture.

The design variables x_i were all normalized between 0 and 1. They are linked to some specific ORC features and are defined by:

$$P_H = P_{crit} - x_1\left(P_{crit} - P_{\min}\right) - 20 \text{ kPa} \tag{3}$$

$$P_I = P_H - x_2\left(P_H - P_{\min}\right) \tag{4}$$

$$P_L = P_I - x_3\left(P_I - P_{\min}\right) \tag{5}$$

$$T_4 = T_{sat}(P_H) + x_4\left(T_{h,i} - \Delta T - T_{sat}(P_H)\right) \tag{6}$$

$$T_6 = T_5 + x_5\left(T_{h,i} - \Delta T - T_5\right) \tag{7}$$

$$T_{h,o} = T_{h,i} - x_6\left(T_{h,i} - \Delta T - T_1\right) \tag{8}$$

$$T_{c,o} = T_{c,i} + x_7\left(T_7 - \Delta T - T_{c,i}\right) \tag{9}$$

$$R_{wf} = x_8\left(R_{wf}\right)_{\max} \tag{10}$$

where ΔT is the minimal temperature difference for heat transfer and P_{crit} is the critical pressure. P_{min} is the minimal possible pressure in the cycle which is determined as the maximum value between saturation pressure at $T_{c,i} + \Delta T$ and 1 atm (101.325 kPa).

The overall energy balance of the black box can be written as:

$$\begin{aligned} &c_{p,h}\left(T_{h,i} - T_{h,o}\right) + R_{wf}\left(h_7 - h_9\right) = \\ &\quad R_{wf}\left(h_4 - h_1\right) + R_{wf}\left(h_6 - h_5\right) + R_c c_{p,c}\left(T_{c,o} - T_{c,i}\right) \end{aligned} \tag{11}$$

This equation was used to calculate R_c so that the overall energy balance was forced. The left-hand side of Eq. (11) accounts for the heat given off by the three hot streams and the right-hand side, the heat taken by the five cold streams. Note that in previous works, instead of an overall energy balance for the black box, several energy balances would be required (one per equipment). Since the internal architecture is not specified here, there is no need for that.

The constraints required to limit the optimization to feasible cycles are thus few in this work. First, vapor quality must be kept to 100% during the expansion in turbines, allowing only dry expansion. Last, all heat exchanges in the HEN must be physically sound, which can be established by the shifting technique, followed by the heat cascade as detailed in [10]. In the present paper, these techniques are referred as to the "cascade method".

The cascade method can be applied not only to determine the heat recovery potential within the system, but also the feasibility of a design. First, thanks to the minimal temperature difference ΔT between the hot and cold streams introduced above, it is possible to define a scaled (shifted) temperature by subtracting $\Delta T/2$ from the temperature of the hot streams and adding $\Delta T/2$ to the temperature of the cold streams. The scaled temperatures of the inlet and outlet of each stream of Fig. 1b can be ordered from the largest to the smallest, defining a series of 13 temperature intervals. For calculation purposes, the temperature of saturated gas states ({3} and {8}) are set as 10^{-5} °C higher than the saturated temperature.

In each interval j, the net enthalpy $h_{net,j}$ is calculated by summing all the available heat (positive value) or needed heat (negative value) by each stream s within these two temperatures, resulting in an excess or deficit of heat:

$$h_{net,j} = \sum_{s=1}^{N} R_s c_{p,s}\left(T_j - T_{j+1}\right) y_{s,j} \tag{12}$$

where c_p is the isobaric specific heat and y is 0 if the stream in not contained in the temperature interval and 1 if it is. N is the number of streams and R is the mass flow rate with respect to the hot source. Thus, in the example, $N = 8$ and R is either 1 (hot source), R_c (cold source) or R_{wf} (working fluid). Note that T is the scaled temperature in the above equation. Then, starting from the highest temperature value, the cascade procedure was applied. This means that

excess heat or heat deficit from this interval is passed and cumulated at the next interval, which is at a lower temperature, and so on, until the lowest temperature is achieved. In this general procedure, heat or cold from external utilities are added when needed. However, in the present case, there are no such utilities. For a situation to be physically sound, it is required that the cumulated cascaded excess energy be positive in each temperature interval. A cycle respecting these features is feasible even though its internal architecture is not exactly known. The cumulative energy becomes:

$$h_{cas,j} = \sum_{k=1}^{j} h_{net,k} \tag{13}$$

In the end, the resulting set of constraints to respect during the optimization can be written as:

$$h_{cas,j} \geq 0 \tag{14}$$

for all intervals j. Note that the last value of the vector h_{cas} should be zero for a feasible design as it corresponds to the overall energy balance of the HEN black box, i.e. Eq. (11). The cascade method thus allows optimizing what is in inside the black box instead of specifying beforehand all the heat exchanges as required by traditional methods.

In summary, the optimization problem for the reheat ORC can be formulated as:

$$\begin{aligned} &\text{maximize: } w \text{ or } \eta_{ex} \\ &\text{by varying: } x_i (i = 1:8) \\ &\text{respecting} \begin{cases} \text{Eq. (14)} \\ \text{Dry expansion only} \end{cases} \end{aligned} \tag{15}$$

The optimization problem was implemented in Matlab and solved with an in-house function based on the Particle Swarm Optimization (PSO) (a metaheuristic developed by Kennedy and Eberhart in 1995 [13]). The PSO control parameters used in this work are: (i) stop criterion: relative error of 10^{-5} between iterations i and $i-3$; (ii) maximum number of iterations: 50; (iii) swarm size: $3{n_{dv}}^3$, where n_{dv} is the number of design variables; (iv) inertia coefficient: 1; (v) damping coefficient: 0.75; (vi) personal acceleration coefficient: 1; (vii) social acceleration coefficient 1.25. Three optimization runs were done systematically for each case, and in the end, the one with the highest value of the objective function was retained.

3. Case 1: Example of results with reheating ORC

The first example employs the reheating ORC (identified as ORC/RH in this work) with ammonia as working fluid, a high efficiency refrigerant recognized as environmentally friendly (ODP = 0 and GWP = 0). The hot source is a pressurized water stream at 140°C, the cold source is a water stream at 15°C, and the minimal temperature difference ΔT is 10°C. The optimization was performed two times, each with a different objective function to compare their respective optimal architecture. The first one maximized the net specific work output w (Eq. (1)), while the second one maximized the exergetic efficiency η_{ex} (Eq. (2)).

Results of both optimization runs are reported in Table 1, showing that the choice of objective function largely influences the outcome. The power output and the exergetic efficiency discrepancies are 19.7% and 7.17%, respectively. Pressure levels are also quite different, and the design maximizing η_{ex} discharges the hot source at a temperature 17.6°C hotter than design maximizing w.

Table 1. Optimization results for the ORC/RH.

Results		Maximizing w	Maximizing η_{ex}
w	[kJ/kg]	27.85	23.26
η_{ex}	[%]	42.37	45.41
P_H	kPa	4644	5992
P_I	kPa	2187	3788
P_L	kPa	1121	1252
T_4	[°C]	113.0	120.6
T_6	[°C]	85.42	95.28
$T_{h,o}$	[°C]	76.17	93.78
$T_{c,o}$	[°C]	18.85	22.42
R_{wf}	[–]	0.1958	0.1486

The information collected in Table 1 can be used to retrieve the optimized HEN architecture. To achieve that, one can position the heat streams in a T-h diagram with the help of the optimal evolutions shown in the T-s diagrams of Fig. 2 (note that the distance between states {9} and {1} (pumping) has been enlarged to ease viewing). Starting with Fig. 2a (maximized w), it first can be seen that the temperature difference between the second turbine outlet (state {7}) and

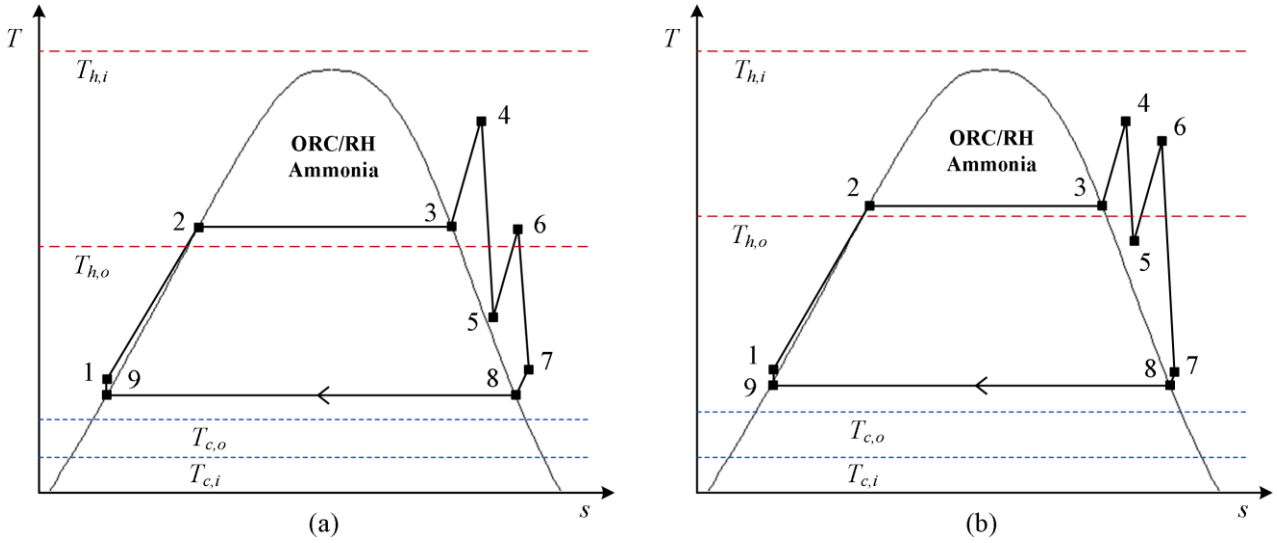

Figure 2. Thermodynamic diagram of optimal design for ORC/RH with maximized (a) specific work output, (b) exergetic efficiency.

the condensation (state {8}) is too small to employ a recuperator, so the cold source must entirely cool down the working fluid from state {7} to {9}. Second, the temperature of state {6} is just below the temperature of the evaporating stream (states {2} to {3}), meaning that the stream in the second superheater SH2 can be heated in parallel with the stream in the economizer EC.

To build the T-h diagram of Fig. 3a, the heat streams can be moved only horizontally, since the zero of the h-axis is arbitrary. The zero enthalpy has been positioned at the hot source outlet, thus $h_{h,o}$ is scaled to zero. Then, the hot and cold sources can easily be placed in the diagram, along with the two streams going through the condenser (states {7} to {9}). The energy balance in the negative enthalpy section verifies that no recuperation was used. Next, in order to generate the architecture, the common method is to start by placing the stream situated at the pinch, and then move away from that point. In the case of a subcritical ORC, the pinch point (minimal temperature difference) is usually at the evaporator input, where the state {h,x} has been added on the hot source in Fig. 3a. Moving to the right, the SH1 working fluid inlet is positioned right after the EV outlet. Energy balance is once more verified by states {h,i} and {4} sharing the same enthalpy value. Finally, the remaining heat from the hot source, i.e., enthalpy of state {h,x} to state {h,o}, is split among the working fluid EC and SH2 streams. Scaled enthalpy of state {h,x} and fraction λ of the hot source flow rate assigned to each streams are:

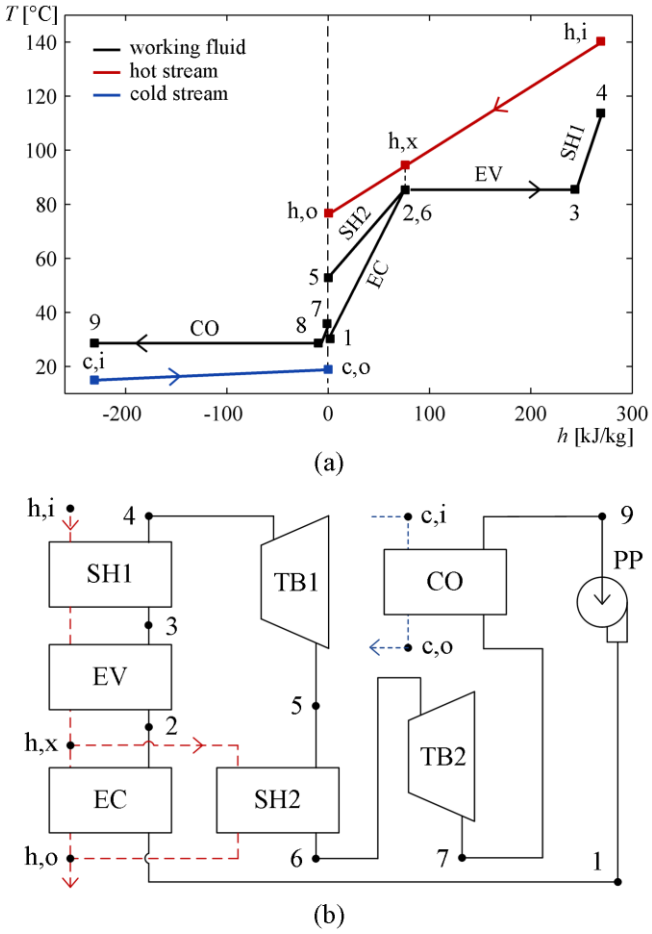

Figure 3. Optimal design for ORC/RH with maximized specific work output (a) Heat exchange diagram. (b) Equipment architecture.

$$h_{h,x} = c_{p,h}\left(T_2 + \Delta T - T_{h,o}\right) \tag{16}$$

$$\lambda_{EC} = \frac{R_{wf}\left(h_2 - h_1\right)}{h_{h,x}}$$
$$\lambda_{SH2} = \frac{R_{wf}\left(h_6 - h_5\right)}{h_{h,x}} \tag{17}$$

where $\lambda_{EC} + \lambda_{SH2} = 1$ when Eq. (14) is respected. The resulting equipment architecture is presented in Fig. 3b, where the hot source is displayed by red dotted lines and the cold source by blue dotted lines. It is the simplest HEN architecture that could be used according to the resulting ORC parameters.

The way to discover the HEN of the design maximizing η_{ex} is similar. Looking at Fig. 2b, one can see there is once more no recuperation possible. The significant difference from earlier is the temperature of state {6} (SH2 outlet) being higher than the evaporating stream temperature in the EV. The hot and cold sources, both condenser streams (states {7} to {9}) and the EV stream can be placed as in Fig. 3a. Then, there is the SH2 stream that can be placed neither left nor right from the EV stream. The simplest solution is to heat this stream in two parts: in the SH2a before the EV until it reaches the highest possible temperature, that is T_2, and next in the SH2b after the EV. Figures 4a and 4b show that the SH2b and SH1 cool in parallel the hot source from state {h,i} to {h,y}, and the SH2a and EC, from state {h,x} to {h,i}. The scaled enthalpy of state {h,y} and the four fractions are:

$$h_{h,y} = h_{h,x} + R_{wf}\left(h_3 - h_2\right) \tag{18}$$

$$\lambda_{EC} = \frac{R_{wf}\left(h_2 - h_1\right)}{h_{h,x}}$$
$$\lambda_{SH2a} = 1 - \lambda_{EC}$$
$$\lambda_{SH1} = \frac{R_{wf}\left(h_4 - h_3\right)}{h_{h,i} - h_{h,o} - h_{h,y}} \tag{19}$$
$$\lambda_{SH2b} = 1 - \lambda_{SH1}$$

Figure 4b is the equipment architecture arising from the T-h diagram. It is slightly more complex than the one in Fig. 3b since it has two separated parallel heat exchange.

The main advantage of the cascade method in ORC design optimization is that there is no need to specify the HEN prior to the design process. In fact, the best internal HEN arises from the optimization, it is not assumed initially as with usual design methods. Furthermore, this proposed approach reduces the number of required assumptions. For example, optimizing an ORC/RH with traditional methods would involve a series of different scenarios of energy balance equations and minimal ΔT verification depending on the position of T_5 and T_6 relative to the evaporation stream temperature.

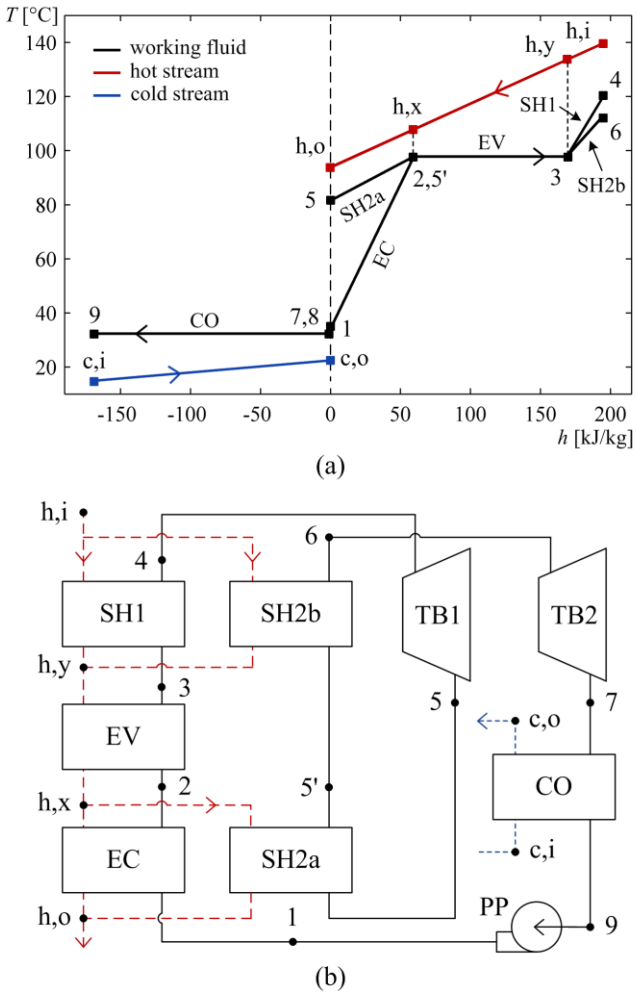

Figure 4. Optimal design for ORC/RH with maximized exergetic efficiency. (a) Heat exchange diagram. (b) Equipment architecture.

4. Case 2: Example of results with dual-pressure ORC

Some power cycles have a "classic" heat exchanger configuration that involves no stream splitting, as for the dual-pressure heating ORC (identified as ORC/DP in this work). Its equipment architecture is shown in Fig. 5. Note that the recuperation has been included in the cycle, recognizable by the recuperator REC. After reaching the intermediate pressure in the first pump PP1 and passing through the REC and first economizer EC1, the working fluid flow rate is separated. A flow rate R_I passes through a series of heat exchangers (EV1 and SH1), and a flow rate R_H is compressed in the second pump PP2 and go through heat exchangers at the cycle highest pressure (EC2, EV2 and SH2). Thus, the flow rate in the second turbine TB2 is R_H,

while it is the total flow $R_H + R_I$ in the first turbine TB1. The expression to calculate the net specific work output is

$$w = \left(R_H + R_I\right)\left[\left(h_{10} - h_{11}\right) - \left(h_1 - h_{13}\right)\right] + R_H\left[\left(h_8 - h_9\right) - \left(h_5 - h_2\right)\right] - \eta_c R_c \left(h_{c,o} - h_{c,i}\right) \quad (20)$$

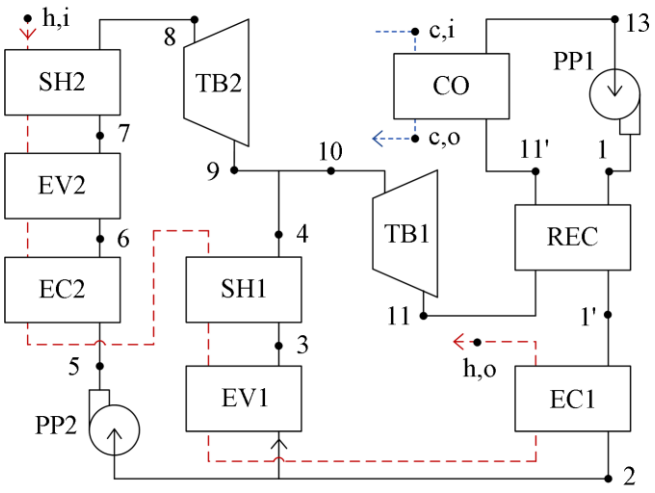

Figure 5. Equipment architecture of typical ORC/DP with recuperation.

This section is about a geothermal power plant in a northern climate exploiting a low-temperature reservoir. The geothermal fluid is considered saturated liquid water at 120°C, the cold source is water at 5°C and the minimal ΔT is 10°C. The working fluid is R1234ze(E), a hydrofluoro-olefin (HFO) with ODP = 0 and GWP < 1. This time, the design variables R_H and R_I take the place of R_{wf} used in Section 3. The net specific work output w (Eq. (20)) is maximized for two cases: using the fixed architecture shown in Fig. 5, and using the cascade method with a "free" HEN. Results are presented in Table 3 and T-s diagrams in Fig. 6.

Table 3. Optimization results for the ORC/DP.

Results		Classic method	Cascade method
w	[kJ/kg]	19.65	27.53
P_H	kPa	2536	2248
P_I	kPa	994.7	1126
P_L	kPa	542.9	425.6
T_4	[°C]	79.82	77.71
T_8	[°C]	96.76	98,44
$T_{h,o}$	[°C]	56.55	53.35
$T_{c,o}$	[°C]	18.42	10.15
R_H	[–]	0.7557	0.8537
R_I	[–]	0.6140	0.5226

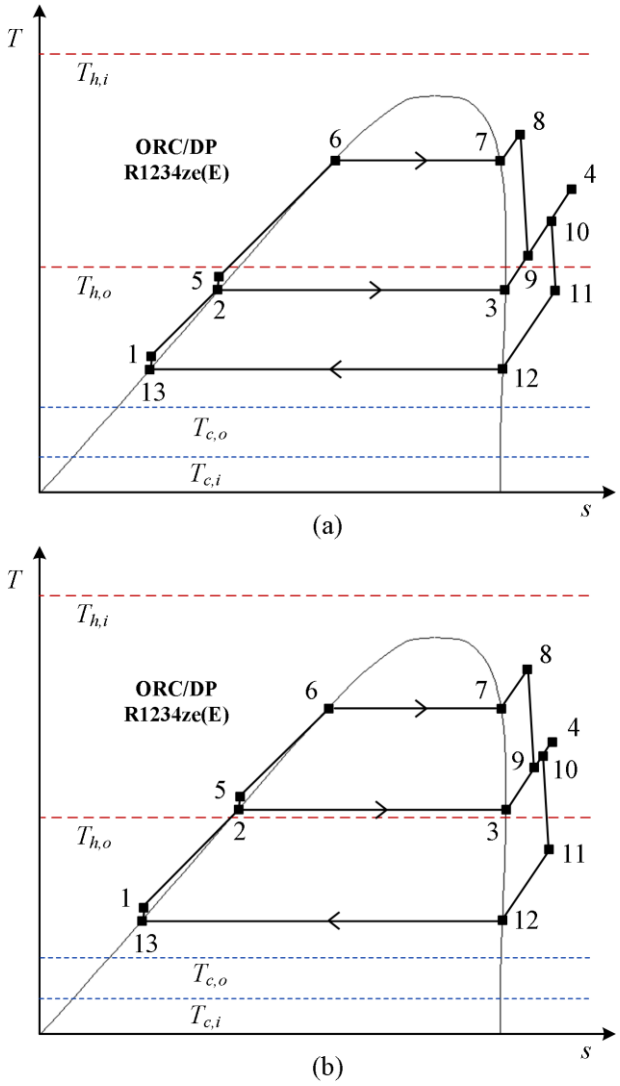

Figure 6. Thermodynamic diagram of optimal ORC/DP design using (a) classic method, (b) cascade method.

The cascade method led to a w 40% higher than the classic method, which is a considerable increase. It tells that the typical architecture is not a fit for this particular case, using R1234ze(E). The notable difference in Fig. 6b is the intermediate pressure being about midway between the low and the high pressure. Figure 7 shows the T-h diagram resulting from the architecture of Fig. 5. Working fluid streams of heat exchangers SH2, EV2, EC2, SH1 and EV1 can be positioned in the diagram, starting from the state {h,i} on the h-axis. Next, the enthalpy of REC outlet states {1'} and {11'} are calculated:

$$h_{11'} = h_{13} - \frac{R_c}{\left(R_H + R_I\right)}\left(h_{c,o} - h_{c,i}\right)$$
$$h_{1'} = h_1 + h_{11} - h_{11'} \quad (21)$$

In the present case, $h_{11'}$ is different than h_{11}, confirming that the REC could be used while respecting the imposed minimal ΔT. Finally, the rest of the streams can be easily placed to complete the T-h diagram.

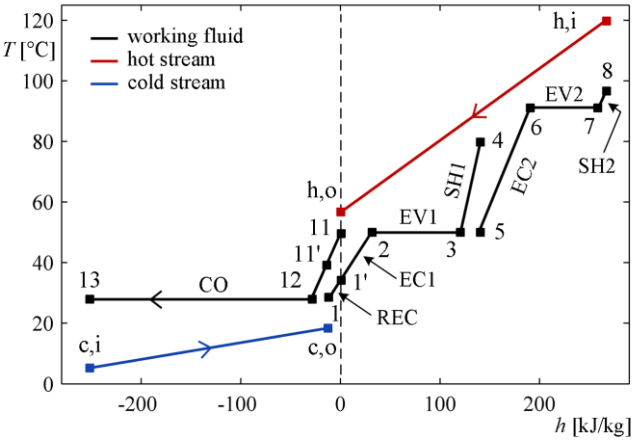

Figure 7. Heat exchange diagram of optimal ORC/DP design using classic method.

A fast way to determine the HEN of the ORC/DP optimized with the cascade method is to first build its T-h diagram considering the typical architecture of Fig. 5. Then, problems like violations of the minimal ΔT or unbalanced heat transfers will guide the modifications to do. In this case, temperature of state {4} (outlet of SH1) does not respect the minimal ΔT with the hot source stream. In Fig. 8a, its scaled enthalpy is thus moved to the right by splitting the hot source stream in two: one stream in the SH1 and the other in the EC2. Scaled enthalpy of states {h,x} and {h,y} and fractions of the hot source are:

$$h_{h,x} = c_{p,h}\left(T_{h,i} - T_{h,o}\right) - R_H\left(h_8 - h_6\right)$$
$$h_{h,y} = h_{h,x} - R_H\left(h_6 - h_5\right) - R_I\left(h_4 - h_3\right) \quad (22)$$

$$\lambda_{EC2} = \frac{R_H\left(h_6 - h_5\right)}{h_{h,x} - h_{h,y}} \quad (23)$$
$$\lambda_{SH1} = 1 - \lambda_{EC2}$$

The resulting architecture is shown in Fig. 8b. It indicates that a simple stream splitting of the hot source between states {h,x} and {h,y} completely changed the HEN performance. This was an example of a case where the typical HEN for ORC/DP limits the net power output. It is worth to mention that in other situations, the resulting HEN could actually be the typical HEN, depending on the working fluid, the nature and temperature of the hot and cold sources, and the chosen minimal ΔT.

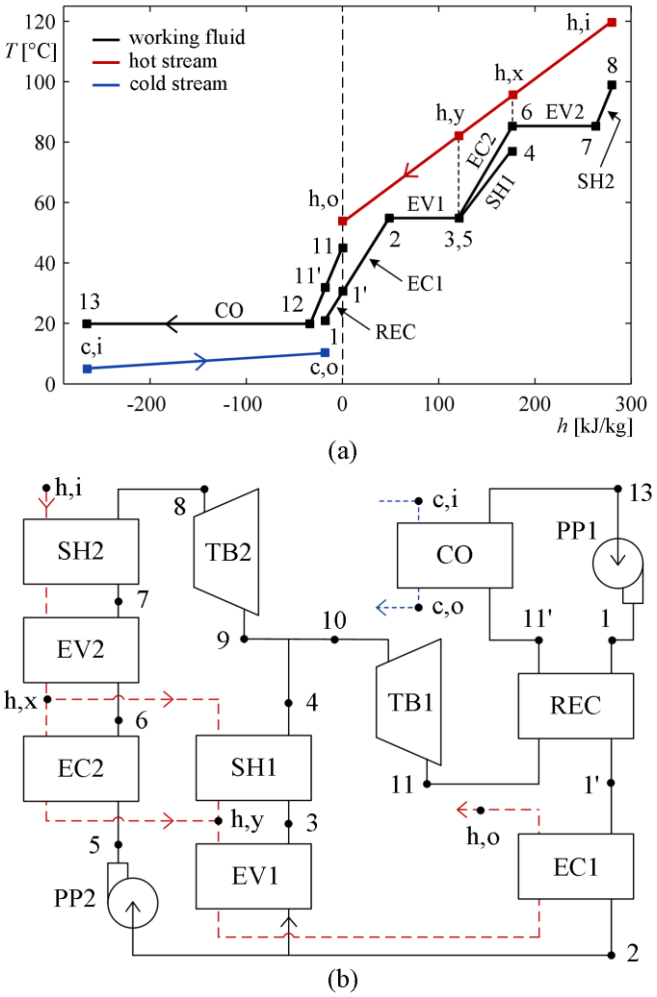

Figure 8. Optimal ORC/DP design using cascade method. (a) Heat exchange diagram. (b) Equipment architecture.

5. Case 3: Example of results for a cement plant

The last example is the application of the ORC as a waste heat recovery system in a cement plant. The data found in [14] on a cement plant indicates that there are two gaseous hot sources released in large amount in the atmosphere, but that can be used for power generation:

1. Preheater exhaust
2. Hot air leaving the cooler

The needed properties are listed in Table 3. The hot sources are assumed not suitable to be mixed into one stream. Flow rates are normalized to totalize 1 kg/s to facilitate calculations and temperatures $T_{h,i}$ are set 50°C colder than where they leave the plant to consider the safe distance between the ORC system and the plant.

Table 3. Values from [14] on the two hot sources.

Parameters		Source 1	Source 2
Flow rate for 3800 tonnes of clinker/day $\dot{m}_h$	[kg/s]	99.88	62.48
Normalized flow rate R_h	[–]	0.615	0.385
Temperature $T_{h,plant}$	[°C]	280	400
Temperature $T_{h,i}$	[°C]	230	350
Specific heat $c_{p,h}$	[kJ/kg·K]	1.0	1.0

In this example, the dual-pressure heater ORC is once more employed, but this time to investigate how the most performant design will distribute the heat from the two available hot sources. The cold source is water at 40°C, the selected working fluid is benzene (a hydrocarbon suitable in the present temperature range with ODP = 0 and GWP = 3) and ΔT is 20°C. The optimization problem is the same as described in Section 4, with the addition of design variables determining both hot sources outlet temperatures $T_{h1,o}$ and $T_{h2,o}$, whose minimum values are set to 120 and 140°C, respectively. The objective function is the specific work output in this example, see Eq. (20). Table 4 displays the optimization results. It was found that both hot sources share the same optimal outlet temperature, and a fairly balanced use of the high-pressure and intermediate-pressure heating was observed, as shown by R_H and R_I. With a net specific work output of 20.21 kJ/kg, the ORC system can deliver a power of 3.3 MW.

Table 4. Optimization results for the ORC/DP using two hot sources.

Parameter		Value
w	[kJ/kg]	20.21
P_H	kPa	2272
P_I	kPa	614.6
P_L	kPa	101.3
T_4	[°C]	152.66
T_8	[°C]	286.82
$T_{h1,o}$	[°C]	151.68
$T_{h2,o}$	[°C]	151.67
$T_{c,o}$	[°C]	50.60
R_H	[–]	0.1051
R_I	[–]	0.1379

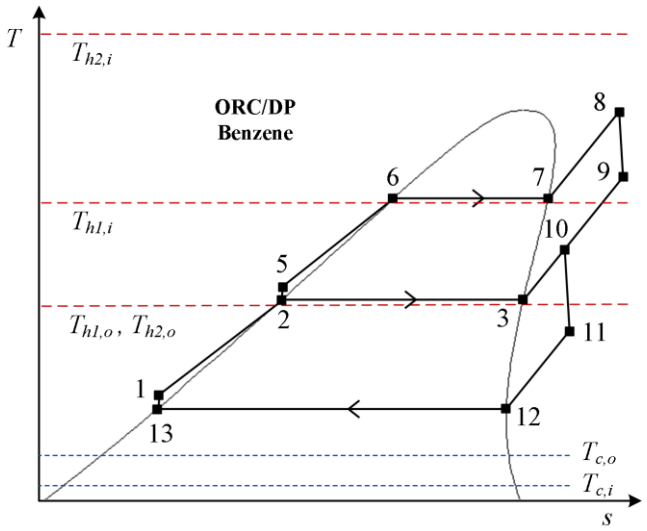

Figure 9. Thermodynamic diagram of optimal ORC/DP design using two hot sources.

Figure 9 shows the T-s diagram of the optimal design. One can see that a recuperator is probably used (large temperature difference between states {11} and {1}), while the intermediate-pressure superheater SH1 is not (state {4} overlays state {3}). In the T-h diagram of Fig. 10a, the cold source, both hot sources (one after the other for more clarity) and both condenser CO streams may first be positioned. Next, the temperature and enthalpy of states {1'} and {11'} are calculated according to Eq. (21) to place the REC stream from states {1} to {1'}. Then, placing the intermediate-pressure evaporator EV1 inlet (state {2}) as near as possible to the first hot source reveals that this hot stream contains not enough energy to heat both the EV1 and EC1 streams. Keeping that in mind, the high-pressure heat exchangers starting with the SH2 stream can be positioned below the second hot source, in order to know what its remaining enthalpy is. It informs that the EV1 and EC1 streams have to be split in two to respect the minimal ΔT in heat exchangers and energy balances. The EC1a and EV1a streams are then heated by the first hot source, and the EC1b and EV1b streams, by the second one. Enthalpy of state {h1,x} is found with Eq. (16) and the needed fractions to calculate scaled enthalpies are:

$$\begin{aligned}
\lambda_{EC1a} &= \frac{\left(R_I + R_H\right)\left(h_2 - h_{1'}\right)}{R_{h,1} h_{h1,x}} \\
\lambda_{EC1b} &= 1 - \lambda_{EC1a} \\
\lambda_{EV1a} &= \frac{R_I \left(h_3 - h_2\right)}{R_{h,1}\left(h_{h1,i} - h_{h1,o} - h_{h1,x}\right)} \\
\lambda_{EV1b} &= 1 - \lambda_{EV1a}
\end{aligned} \tag{24}$$

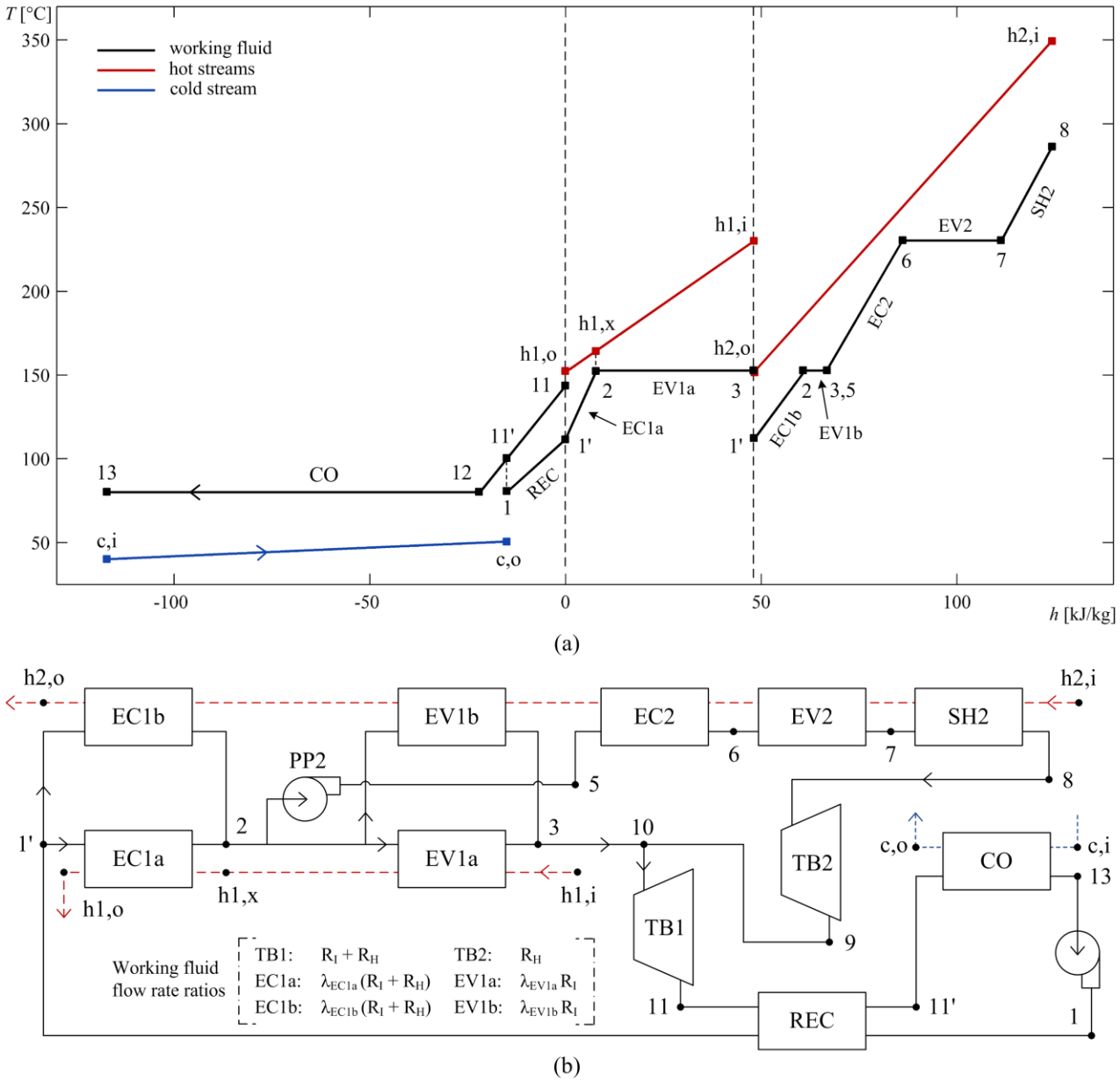

Figure 10. Optimal design for ORC/DP using two hot sources. (a) Heat exchange diagram. (b) Equipment architecture.

Figure 10b is the equipment architecture created from the T-h diagram of Fig. 10a. This design maximizes the specific work output of the ORC system and does not take into account economic aspects related to the cost of the equipment.

The case presented in this section shows that using the cascade method can help to design high performance ORCs by enabling the exploration of more complex systems that would normally have been challenging to optimize.

6. Conclusion

The purpose of this paper was to introduce a way to optimize ORCs where the heat exchanger network (HEN) would self-generate, rather than having to be assumed. This was found to be possible with the cascade method that allows cascading the excess heat down to lower temperatures. Three different cases showed the benefits of using the cascade method over the "normal" method.

It was observed that heat exchange assumptions that are normally needed to ensure energy balances with traditional

design methods tend to limit the design optimization. The first example showed that leaving all the heat exchange "free" to verify the global energy balance in one step allows to get rid of these assumptions. The second example demonstrated that using the cascade method can self-generate a more performant HEN than the conventional design method, leading to 40% more power produced in this case. In the third example, a waste heat recovery case from two hot sources revealed how easily a more complex system can be handled by letting the optimization choose the best HEN.

This work could be extended in numerous manners. For example, other ORC configurations could be explored, like transcritical cycles. A possible next step is to perform optimization runs for wide ranges of hot and cold sources inlet temperatures and for various working fluids, including mixtures of fluids, to develop guidelines and decision-making diagrams. Finally, economic aspects could be considered by making a multi-objective optimization including the cost as an objective function besides the thermodynamic performance.

ACKNOWLEDGMENTS

This work was supported by the Natural Sciences and Engineering Research Council of Canada (NSERC).

REFERENCES

[1] "Waste Heat: Innovators Turn to an Overlooked Renewable Resource," *Yale E360*. [Online]. Available: https://e360.yale.edu/features/waste-heat-innovators-turn-to-an-overlooked-renewable-resource. [Accessed: 07-Oct-2019].

[2] S. Quoilin, M. V. D. Broek, S. Declaye, P. Dewallef, and V. Lemort, "Techno-economic survey of Organic Rankine Cycle (ORC) systems," *Renew. Sustain. Energy Rev.*, vol. 22, pp. 168–186, Jun. 2013.

[3] N. Chagnon-Lessard, F. Mathieu-Potvin, and L. Gosselin, "Geothermal power plants with maximized specific power output: Optimal working fluid and operating conditions of subcritical and transcritical Organic Rankine Cycles," *Geothermics*, vol. 64, pp. 111–124, Nov. 2016.

[4] P. J. Mago, L. M. Chamra, K. Srinivasan, and C. Somayaji, "An examination of regenerative organic Rankine cycles using dry fluids," *Appl. Therm. Eng.*, vol. 28, no. 8, pp. 998–1007, Jun. 2008.

[5] K. Braimakis and S. Karellas, "Energetic optimization of regenerative Organic Rankine Cycle (ORC) configurations," *Energy Convers. Manag.*, vol. 159, pp. 353–370, Mar. 2018.

[6] Y. A. Çengel, M. A. Boles, and M. Lacroix, *Thermodynamique: Une Approche Pragmatique*, Sixth. Montréal: Les Éditions de la Chenelière inc., 2008.

[7] M. Wang, Y. Chen, Q. Liu, and Z. Yuanyuan, "Thermodynamic and thermo-economic analysis of dual-pressure and single pressure evaporation organic Rankine cycles," *Energy Convers. Manag.*, vol. 177, pp. 718–736, Dec. 2018.

[8] A. Lazzaretto and A. Toffolo, "A method to separate the problem of heat transfer interactions in the synthesis of thermal systems," *Energy*, vol. 33, no. 2, pp. 163–170, Feb. 2008.

[9] A. Toffolo, A. Lazzaretto, G. Manente, and M. Paci, "A multi-criteria approach for the optimal selection of working fluid and design parameters in Organic Rankine Cycle systems," *Appl. Energy*, vol. 121, pp. 219–232, May 2014.

[10] R. Smith, *Chemical Process: Design and Integration*. Chichester: John Wiley & Sons, Ltd, 2005.

[11] N. Chagnon-Lessard, F. Mathieu-Potvin, and L. Gosselin, "Optimal design of geothermal power plants: A comparison of single-pressure and dual-pressure Organic Rankine Cycles," (submitted) 2019.

[12] A. Bejan, *Advanced Engineering Thermodynamics*, Fourth edition. Hoboken: John Wiley & Sons, Inc., 2016.

[13] J. Kennedy and R. Eberhart, "Particle swarm optimization," in *, IEEE International Conference on Neural Networks, 1995. Proceedings*, 1995, vol. 4, pp. 1942–1948 vol.4.

[14] S. Khurana, R. Banerjee, and U. Gaitonde, "Energy balance and cogeneration for a cement plant," *Appl. Therm. Eng.*, vol. 22, no. 5, pp. 485–494, Apr. 2002.